Glycolysis controls the induction of human regulatory T cells by modulating the expression of *FOXP3* exon 2 splicing variants

Veronica De Rosa,

Laboratorio di Immunologia, Istituto di Endocrinologia e Oncologia Sperimentale, Consiglio Nazionale delle Ricerche, Napoli, Italy. Unità di NeuroImmunologia, Fondazione Santa Lucia, Roma, Italy

Mario Galgani,

Laboratorio di Immunologia, Istituto di Endocrinologia e Oncologia Sperimentale, Consiglio Nazionale delle Ricerche, Napoli, Italy

Antonio Porcellini,

Dipartimento di Biologia, Complesso Universitario di Monte Sant'Angelo, Università di Napoli "Federico II", Napoli, Italy

Alessandra Colamatteo,

Unità di NeuroImmunologia, Fondazione Santa Lucia, Roma, Italy. Dipartimento di Medicina e Chirurgia, Università di Salerno, Baronissi Campus, Baronissi, Salerno, Italy

Marianna Santopaolo,

Dipartimento di Medicina Molecolare e Biotecnologie Mediche, Università di Napoli "Federico II", Napoli, Italy

Candida Zuchegna,

Dipartimento di Biologia, Complesso Universitario di Monte Sant'Angelo, Università di Napoli "Federico II", Napoli, Italy

Antonella Romano,

Dipartimento di Biologia, Complesso Universitario di Monte Sant'Angelo, Università di Napoli "Federico II", Napoli, Italy

Salvatore De Simone,

Laboratorio di Immunologia, Istituto di Endocrinologia e Oncologia Sperimentale, Consiglio Nazionale delle Ricerche, Napoli, Italy

Claudio Procaccini,

Corresponding author: Giuseppe Matarese: gmatarese@unisa.it.

Laboratorio di Immunologia, Istituto di Endocrinologia e Oncologia Sperimentale, Consiglio Nazionale delle Ricerche, Napoli, Italy

Claudia La Rocca,
Laboratorio di Immunologia, Istituto di Endocrinologia e Oncologia Sperimentale, Consiglio Nazionale delle Ricerche, Napoli, Italy

Pietro Biagio Carrieri,
Dipartimento di Neuroscienze e Scienze Riproduttive ed Odontostomatologiche, Università di Napoli "Federico II", Napoli, Italy

Giorgia Teresa Maniscalco,
Dipartimento di Neurologia, Centro Regionale Sclerosi Multipla, Azienda Ospedaliera "A. Cardarelli", Napoli, Italy

Marco Salvetti,
Centro Neurologico Terapie Sperimentali, Dipartimento di Neuroscienze, Salute Mentale e Organi di Senso, "Sapienza" Università di Roma, Roma, Italy

Maria Chiara Buscarinu,
Centro Neurologico Terapie Sperimentali, Dipartimento di Neuroscienze, Salute Mentale e Organi di Senso, "Sapienza" Università di Roma, Roma, Italy

Adriana Franzese,
Dipartimento di Scienze Mediche Traslazionali, Università di Napoli "Federico II", Napoli, Italy

Enza Mozzillo,
Dipartimento di Scienze Mediche Traslazionali, Università di Napoli "Federico II", Napoli, Italy

Antonio La Cava, and
Department of Medicine, David Geffen School of Medicine, University California of Los Angeles, Los Angeles, California, USA

Giuseppe Matarese
Dipartimento di Medicina e Chirurgia, Università di Salerno, Baronissi Campus, Baronissi, Salerno, Italy. Istituto di Ricovero e Cura a Carattere Scientifico MultiMedica, Milano, Italy

Abstract

Human regulatory T cells (T_{reg} cells) that develop from conventional T cells (T_{conv} cells) following suboptimal stimulation via the T cell antigen receptor (TCR) (induced T_{reg} cells (iT_{reg} cells)) express the transcription factor Foxp3, are suppressive, and display an active proliferative and metabolic state. Here we found that the induction and suppressive function of iT_{reg} cells tightly depended on glycolysis, which controlled *Foxp3* splicing variants containing exon 2 (Foxp3-E2) through the glycolytic enzyme enolase-1. The Foxp3-E2–related suppressive activity of iT_{reg} cells was altered in human autoimmune diseases, including multiple sclerosis and type 1 diabetes, and was associated with impaired glycolysis and signaling via interleukin 2. This link between glycolysis and Foxp3-E2 variants via enolase-1 shows a previously unknown mechanism for controlling the induction and function of T_{reg} cells in health and in autoimmunity.

Introduction

Distinct subsets of $CD4^+CD25^+$ human regulatory T cells (T_{reg} cells) are involved in the maintenance of immunological self-tolerance and the control of autoimmunity[1]. T_{reg} cells are classified into two main subgroups according to their developmental origin, and both express the transcription factor Foxp3 (refs. 2,3). One subgroup arises from the thymus as a distinct lineage, and the other subgroup derives from the peripheral conversion of $CD4^+CD25^-$ conventional T cells (T_{conv} cells)[4, 5]. Experimental evidence indicates that T_{reg} cell differentiation relies on multiple signaling pathways, such as those derived from the cytokine milieu, engagement of the T cell antigen receptor (TCR), the costimulatory molecule CD28, and signaling via interleukin 2 (IL-2) and its receptor (IL-2R). For example, the cytokine TGF-β can induce Foxp3 expression in T_{conv} cells stimulated via the TCR, which leads to their conversion into inducible T_{reg} cells (iT_{reg} cells) with strong *in vitro* suppressive capacity[6, 7]. Additionally, chronic activation of $CD4^+$ T cells in the presence of TGF-β can induce the differentiation of a T_{reg} cell subset that suppresses antigen-specific T cell responses in both mice and humans[6, 7]. However, cytokines can be dispensable in the generation of human iT_{reg} cells, as these cells can also be generated by *in vitro* stimulation of T_{conv} cells in a cytokine-independent manner[8, 9]. In this context, homeostatic proliferation of T_{conv} cells *in vivo* can produce a population of $CD25^+$ T cells with low proliferative capacity and the ability to suppress antigen-specific T cell responses[10]. *In vitro* and *in vivo* studies have shown that the extent of signaling via the TCR and associated costimulatory molecules can affect the outcome of T cell differentiation[11, 12]. In this context, culture of $CD4^+$ T cells in the presence of dendritic cells presenting low concentrations of antigen results in T_{reg} cell proliferation together with the conversion of T_{conv} cells into iT_{reg} cells[13]. Therefore, the density and affinity of TCR ligation seem to control the induction of Foxp3, since maximal TCR stimulation seems to be detrimental to the differentiation of T_{reg} cells, whereas optimal induction of Foxp3 is associated with suboptimal TCR engagement[14, 15]. Accordingly, antigen-specific T_{reg} cells can be induced efficiently in mice when an agonist peptide is administered in sub-immunogenic doses, as supra-physiological stimulation leads to the proliferation of $CD4^+CD25^+$ T cells without Foxp3 expression[16].

Distinct metabolic pathways control the function and differentiation of T cells[17, 18, 19]. The activation of $CD4^+$ T cells requires metabolic reprogramming characterized by diminished lipid oxidation and increased glycolysis[17, 18, 19]. Metabolic enzymes can influence T cell fate by modulating both lineage-specific differentiation and cytokine production[20, 21]. Here we found that highly suppressive human iT_{reg} cells were generated in the absence of exogenous regulatory-type cytokines (i.e., TGF-β or IL-10) following suboptimal stimulation of T_{conv} cells via the TCR. They represented the highly glycolytic and metabolically active fraction of proliferating T_{conv} cells and depended for their induction on the expression of *Foxp3* splicing variants containing exon 2 (*Foxp3*-E2). Among all splicing variants of human Foxp3, the variant produced from *FOXP3*-E2 (called 'Foxp3-E2' here) has been shown to serve a major role in conferring suppressive ability onto T_{reg} cells[22, 23, 24]. Therefore, we focused on the metabolic determinants that led to the induction of Foxp3-E2 in human iT_{reg} cells and found that glycolysis controlled the generation of iT_{reg} cells through localization of the glycolytic enzyme enolase-1 to the nucleus. Enolase-1

directly affected the expression of Foxp3-E2 after binding to *FOXP3* regulatory regions, such as the promoter and conserved noncoding sequence 2 (CNS2). We confirmed our findings in studies of subjects with the autoimmune diseases relapsing-remitting multiple sclerosis (RRMS) or type 1 diabetes (T1D), in whom we observed impaired glycolysis and Foxp3-E2 expression in iT_{reg} cells.

Results

Generation of iT_{reg} cells after suboptimal TCR stimulation

To determine whether the induction of human iT_{reg} cells from T_{conv} cells could be achieved through weak stimulation of the TCR in the absence of exogenous cytokines, we obtained peripheral blood mononuclear cells (PBMCs) from healthy human subjects, negatively selected T_{conv} cells (purity, >98%) from those cells and activated them (via the TCR) for 36 h *in vitro* with beads coated with monoclonal antibody (mAb) to the invariant signaling protein CD3 plus mAb to CD28 (at a density of 0.1 bead per cell) (Supplementary Fig. 1). At 24 h after activation, we assessed cellular metabolism (glycolysis, mitochondrial respiration and fatty acid oxidation (FAO)) by measuring the extracellular acidification rate (ECAR) and oxygen-consumption rate (OCR). T_{conv} cells underwent an increase in their mitochondrial respiration rate (OCR) and used both glucose and fatty acids, as indicated by an increase in glycolysis and FAO (Fig. 1a, b). At 36 h after activation, we sorted T_{conv} cells by flow cytometry into three subsets on the basis of their cell-surface expression of the T cell–activation marker CD25. We subsequently assessed the proliferation marker Ki67, phosphorylation of S6 (a downstream target of the metabolic checkpoint kinase mTOR) and Foxp3 in cells with high CD25 expression ($CD25^{hi}$), intermediate CD25 expression ($CD25^{int}$) or low CD25 expression ($CD25^{lo}$) and found that $CD25^{hi}$ cells had highest levels of all these (Fig. 1c). In parallel, we evaluated the ability to suppress *in vitro* the proliferation of $CD4^+$ T cells labeled with the division-tracking dye CFSE and stimulated with mAb to CD3 plus mAb to CD28. We found that the subset with the highest expression of CD25, Ki67 and Foxp3 and greatest phosphorylation of S6 also had the strongest suppressive activity (Fig. 1d) and that the suppression was contact dependent (Supplementary Fig. 2a). We also evaluated the methylation status of *FOXP3* CNS2 to assess the stability of *FOXP3* expression (a more highly methylated CNS2 is related to diminished stability). The frequency of CNS2 methylation in iT_{reg} cells was low and similar to that observed in freshly isolated T_{reg} cells (Supplementary Fig. 2b). The low CNS2-methylation status, high suppressive activity and expression of T_{reg} cell–characteristic surface markers (CTLA-4, PD-1, GITR and CD71) were retained for up to 10 d of culture in the presence of IL-2, at levels similar to those of the initially generated iT_{reg} cells (at 36 h) (Supplementary Fig. 2b–d). The generation of iT_{reg} cells did not depend on TGF-β and IL-10, since neutralization of these cytokines *in vitro* did not alter the induction of iT_{reg} cells (data not shown). These results indicated that human iT_{reg} cells could be induced from T_{conv} cells stimulated by weak engagement of TCR in the absence of exogenous cytokines and that they retained their suppressive capacity overtime.

Glycolysis and FAO in the generation and function of iT_{reg} cells

Since the generation and function of T cells depend on underlying metabolic programs[17, 18, 19], we evaluated the metabolic pathways involved in the generation of iT_{reg} cells. We activated T_{conv} cells in the presence or absence of a specific inhibitor of glycolysis (2-deoxy-D-glucose (2DG)) and a specific inhibitor of FAO (etomoxir (Etx)) (Supplementary Fig. 3). 2DG-treated T_{conv} cells had lower glycolysis than that of untreated T_{conv} cells and had mitochondrial respiration (Fig. 2a) and FAO (Fig. 2b) similar to that of untreated T_{conv} cells. In contrast, treatment with Etx affected the FAO rate (Fig. 2b) and decreased the mitochondrial respiration without any substantial effect on glycolysis (Fig. 2a). Although both compounds inhibited the upregulation of CD25 expression, Foxp3 expression was much lower in CD25^{hi} T cells generated in the presence of 2DG and sorted by flow cytometry (iT_{reg}-2DG cells) and was higher in sorted CD25^{hi} T cells generated in the presence of Etx (iT_{reg}-Etx cells) than in untreated (control (CTR)) CD25^{hi} T cells (iT_{reg}-CTR cells) (Fig. 2c). To determine whether the metabolic perturbations were associated with an altered regulatory function, we assessed the ability of iT_{reg}-2DG cells and iT_{reg}-Etx cells to suppress the proliferation of CD4$^+$ T cells *in vitro*. iT_{reg}-2DG cells displayed less suppressive function than that of iT_{reg}-CTR cells, whereas iT_{reg}-Etx cells had higher suppressive activity than that of iT_{reg}-CTR cells (Fig. 2d). Together these results indicated that glycolysis was necessary for the generation and suppressive function of human iT_{reg} cells.

Biochemical signature of iT_{reg} cells

To better understand the molecular basis of the findings reported above for iT_{reg} cells, we studied cell metabolism, cytokine-related signaling and Foxp3 expression during specific metabolic perturbations. Immunoblot analysis of iT_{reg} cells stimulated *in vitro* for 1 h with mAb to CD3 plus mAb to CD28 showed that both 2DG and Etx reduced the activation of mTOR in iT_{reg} cells, in terms of the phosphorylation of S6, but via different mechanisms (Fig. 3). Indeed, while 2DG abolished the phosphorylation of S6, Etx increased the total amount of S6 without increasing its activity in terms of phosphorylation. Moreover, iT_{reg}-2DG cells had lower expression of enolase-1 than that of iT_{reg}-CTR cells, whereas iT_{reg}-Etx cells had enolase-1 expression similar to that of iT_{reg}-CTR cells. Also, iT_{reg}-2DG cells had less phosphorylation of the signal transducer STAT3 than that of iT_{reg}-CTR cells, whereas iT_{reg}-Etx cells had an amount of STAT3 phosphorylation similar to that of iT_{reg}-CTR cells. The IL-2–IL-2R–STAT5 signaling pathway has a central role in the induction of Foxp3 and in the generation and homeostasis of T_{reg} cells[25, 26]. We found profound impairment in the activation of STAT5 in iT_{reg}-2DG cells following TCR stimulation, whereas the induction of STAT5 phosphorylation was greater in stimulated iT_{reg}-Etx cells than in their iT_{reg}-CTR counterparts.

Human Foxp3 has various splicing variants; however, despite the importance of Foxp3 in T_{reg} cells, the regulation and functional activity of Foxp3 isoforms remain poorly understood[22, 23, 24]. Since we observed that glycolysis was necessary for the induction of human iT_{reg} cells, we evaluated the differential effects of metabolic perturbations on Foxp3 isoforms. Specifically, we found that 2DG hampered induction of the 47-, 44- and 38-kilodalton (kDa) forms of Foxp3 but favored expression of the 49-kDa form (Fig. 3). In

contrast, Etx increased the expression of the 47-kDa form but did not affect the expression of the 49-, 44- or 38-kDa forms (Fig. 3). Of note, the densitometric sum of total Foxp3 forms showed no difference among the three iT_{reg} cell populations (Fig. 3), which suggested differential metabolic regulation of the various splicing forms of Foxp3 in iT_{reg} cells. We confirmed these data at the mRNA level by RT-PCR analysis (data not shown). Overall, these analyses revealed that glycolysis controlled the generation of human iT_{reg} cells via a specific biochemical machinery involving the mTOR pathway, IL-2R signaling and the modulation of various splicing variants of Foxp3.

Metabolic programs and phenotypical characteristics of iT_{reg} cells

Next we evaluated the phenotype and the metabolic profile of iT_{reg} cells generated in the presence of inhibitors of either glycolysis or FAO. Inhibition of glycolysis with 2DG diminished expression of the T_{reg} cell markers CTLA-4, PD-1, GITR, CD39 and CD71, as well as the phosphorylation of S6, whereas Etx had an effect similar to that of 2DG on the expression of PD-1 and CD39 and phosphorylation of S6, but slightly reduced the expression of CD71 and CCR7, preserved the expression of CTLA-4, and upregulated the expression of GITR, compared with results obtained with no treatment (in iT_{reg}-CTR cells) (Fig. 4a). The measurement of ECAR (glycolysis) and OCR (FAO and oxidative phosphorylation) in iT_{reg} cells indicated that iT_{reg}-2DG cells had impaired glycolysis and mitochondrial respiration relative to that of iT_{reg}-CTR cells (Fig. 4b), with FAO rates similar to those of iT_{reg}-CTR cells (Fig. 4c). Etx affected FAO (Fig. 4c) and mitochondrial respiration (Fig. 4b) but preserved glycolysis (Fig. 4b), relative to results obtained with no treatment (in iT_{reg}-CTR cells). These effects, secondary to the metabolic perturbations, were not associated with altered survival and/or viability of T cells, as indicated by staining with propidium iodide and annexin V, which was similar in iT_{reg}-2DG, iT_{reg}-Etx and iT_{reg}-CTR cells (data not shown). Thus, inhibition of glycolysis impaired the generation and function of iT_{reg} cells and reduced the induction of Foxp3 and the expression of T_{reg} cell markers.

Glycolysis controls iT_{reg} cells' suppressive function via Foxp3-E2

To better understand the effects of metabolism on the expression of the splicing variants of Foxp3, as they were related to the regulatory function of iT_{reg} cells, we analyzed, at level of both mRNA and protein, the expression of all *FOXP3* transcripts and that of the two main *FOXP3* spliced forms[22, 23, 24, 26]: one containing exon 2 (*FOXP3*-E2), and the other lacking it (Fig. 5a). Quantitative RT-PCR with primers spanning exons 9–11 (to amplify all transcripts) showed a 37-fold greater abundance of total *FOXP3* mRNA in iT_{reg}-CTR cells than in T_{conv} cells (Fig. 5b). iT_{reg}-2DG cells had 50% less total *FOXP3* mRNA, whereas iT_{reg}-Etx cells had very slightly but significantly greater levels of total *FOXP3* mRNA, than iT_{reg}-CTR cells had (Fig. 5b). Quantitative RT-PCR with specific primers for the amplification of transcripts containing *FOXP3* exon 2 (Fig. 5a) showed that the expression of *FOXP3*-E2 mRNA was twofold lower in iT_{reg}-2DG cells and 1.4-fold higher in iT_{reg}-Etx cells than in iT_{reg}-CTR cells (Fig. 5b).

To further assess whether 2DG and Etx regulated the splicing of exon 2 differentially, we did semiquantitative RT-PCR with primers spanning exons 1–3. 2DG affected only the expression of *FOXP3*-E2, whereas Etx increased the abundance of both *FOXP3*-E2 and

FOXP3 lacking exon 2 compared with results obtained for untreated (iT$_{reg}$-CTR) cells (Fig. 5b). Next we sought to determine whether level of mRNA from the *FOXP3* splicing forms correlated with protein expression in iT$_{reg}$ cells generated in the presence of metabolic inhibitors. For this, we measured all splicing forms of Foxp3 protein by using two specific mAbs: one (PCH101) that recognizes all splicing variants of Foxp3 (through a common epitope of the amino terminus of Foxp3); the other (150D/E4) specific for the variants encoded by *FOXP3*-E2 (recognized through an epitope encoded by sequence present only in exon 2). Immunoblot analysis with mAb PCH101 revealed that the amount of the 49-kDa form of Foxp3 increased after treatment with each metabolic inhibitor, relative to its abundance in untreated (iT$_{reg}$-CTR) cells, with this phenomenon being more evident in iT$_{reg}$-2DG cells (Fig. 5c). iT$_{reg}$-2DG cells had substantially less of both the 47-kDa splicing form and 44-kDa splicing form than iT$_{reg}$-CTR cells had, whereas the level of these forms was not altered in iT$_{reg}$-Etx cells relative to that in iT$_{reg}$-CTR cells (Fig. 5c). The densitometric sum of the various Foxp3 splicing forms showed no difference among the three iT$_{reg}$ cell populations (Fig. 5c), which indicated that the effects induced by the metabolic inhibitors were specific for defined splicing variants of Foxp3.

To determine whether the lower abundance of the 44- to 47-kDa splicing forms had to be ascribed to a lower abundance of *FOXP3*-E2 (as observed by quantitative RT-PCR), we performed immunoblot analysis of the same cell lysates with mAb 150D/E4 to the variants encoded by *FOXP3*-E2 (Foxp3-E2), which detects a 47-kDa product. iT$_{reg}$-2DG cells had much less Foxp3-E2, whereas iT$_{reg}$-Etx cells had more Foxp3-E2, than iT$_{reg}$-CTR cells had (Fig. 5c). Flow cytometry confirmed that treatment with 2DG led to the generation of iT$_{reg}$ cells with reduced expression of Foxp3, both as total Foxp3 and Foxp3-E2, whereas Etx increased both total Foxp3 and Foxp3-E2 in iT$_{reg}$ cells, relative to their expression in untreated (iT$_{reg}$-CTR) cells (Supplementary Fig. 4a), and that these effects were dose dependent (Supplementary Fig. 4b, c). Thus, glycolysis and FAO controlled the expression of splicing variants of Foxp3 in iT$_{reg}$ cells differentially, at the level of both mRNA and protein.

Since iT$_{reg}$-2DG cells displayed impaired suppressive capacity associated with reduced expression of Foxp3-E2, with the region of Foxp3 encoded by exon 2 being part of the Foxp3 transcriptional repressor domain[22, 23, 24], we studied whether Foxp3-E2 was indispensable for the regulatory function of iT$_{reg}$ cells by using small interfering mRNA (siRNA) specific for the *FOXP3*-E2 domain (siRNA-E2). We generated iT$_{reg}$ cells in the presence of siRNA-E2 and assessed their ability to suppress the proliferation of CD4$^+$ T cells *in vitro*. After confirming, by immunoblot analysis, siRNA-induced silencing in T$_{conv}$ cells stimulated with mAb to CD3 plus mAb to CD28 (Supplementary Fig. 5a), we found that iT$_{reg}$ cells generated in the presence of siRNA-E2 had less suppressive ability than iT$_{reg}$ cells generated in the presence of control siRNA with a scrambled sequence (siRNA-Scr) (Fig. 5d), despite the finding that iT$_{reg}$ cells generated in the presence of siRNA-E2 expressed the other Foxp3 splice variants (44 kDa) (Supplementary Fig. 5a). Of note, iT$_{reg}$ cells generated in the presence of siRNA-E2 had an impaired suppressive phenotype (Fig. 5d) similar to that of iT$_{reg}$-2DG cells (Fig. 2d). As an additional control, we also silenced *FOXP3* exon 5, a common sequence for all *FOXP3* transcripts, with siRNA (siRNA- E5); this reduced the abundance of all the *FOXP3* splicing variants (Supplementary Fig. 5a) and

markedly hampered the generation of iT$_{reg}$ cells, as indicated by the substantial reduction in CD25 expression (data not shown). iT$_{reg}$ cells generated in the presence of siRNA-E5, sorted on the basis of their CD25^{hi} phenotype, had a suppressive ability similar to that of iT$_{reg}$ cells generated in the presence of siRNA-Scr (Fig. 5d). These phenomena occurred because silencing of *FOXP3* exon 5 reduced the induction of all *FOXP3* splicing variants and, consequently, hampered the upregulation of CD25 expression and the generation of iT$_{reg}$ cells (data not shown). Since the sorting gate was on CD25^{hi} cells, it was likely that CD25^{hi} cells recovered from the silencing of *FOXP3* exon 5 were those in which the knockdown had failed, which had retained their suppressive ability (Fig. 5d). Overall, these analyses revealed that glycolysis controlled the expression of Foxp3-E2, which was necessary for the suppressive function of human iT$_{reg}$ cells.

Enolase-1 controls Foxp3-E2 expression

Several isoforms of enolase-1, a key glycolytic enzyme, can bind DNA[27, 28, 29]. Among them, the 37-kDa isoform (MBP-1) has been shown to regulate gene expression in various experimental systems[27, 28, 29]. Both the glycolytic enzyme enolase-1 and the transcriptional repressor MBP-1 arise from the gene *ENO1* through the use of alternative translation start sites present on *ENO1* mRNA[29, 30]. Published evidence suggests that enolase-1 isoforms have multifunctional roles, ranging from glycolytic activity in the cytoplasm to gene regulation in the nucleus[29, 30]. For this reason, we evaluated whether enolase-1 isoforms localized in the nuclear fraction of iT$_{reg}$-CTR, iT$_{reg}$-2DG and iT$_{reg}$-Etx cells to control *FOXP3* expression. Immunoblot analysis revealed that three different products of the alternative translation start sites of the *ENO1* transcript (48, 37 and 31 kDa in size) were selectively greater in abundance in iT$_{reg}$-2DG cells than in iT$_{reg}$-CTR cells, whereas their amounts were similar in iT$_{reg}$-Etx cells and iT$_{reg}$-CTR cells (Fig. 6a). To determine whether enolase-1 was involved in the regulation of *FOXP3* in iT$_{reg}$ cells, we first evaluated the binding of enolase-1 to the *FOXP3* regulatory elements and then assessed the effect of the silencing of *ENO1* on *FOXP3* mRNA expression. Chromatin-immunoprecipitation analysis revealed that the recruitment of enolase-1 to both the *FOXP3* promoter and its CNS2 regions was greater in iT$_{reg}$-2DG cells than in iT$_{reg}$-CTR cells (Fig. 6b); in contrast, the association of enolase-1 with the *FOXP3* promoter was much lower in iT$_{reg}$-Etx cells than in iT$_{reg}$-CTR cells, but its association with *FOXP3* CNS2 was similar in iT$_{reg}$-Etx cells and iT$_{reg}$-CTR cells (Fig. 6b). Freshly isolated, unstimulated T$_{conv}$ cells, which did not express Foxp3, had less cytoplasmic enolase-1 than did iT$_{reg}$-CTR cells, and the recruitment of enolase-1 to the *FOXP3* regulatory elements in these cells was similar to that in iT$_{reg}$-2DG cells (Supplementary Fig. 5b and Fig. 6b).

To address whether enolase-1 directly controlled the splicing of *FOXP3* mRNA, we silenced *ENO1* by using ENO1-specific siRNA (siRNA-ENO1) during the generation of iT$_{reg}$ cells. After confirmation by quantitative RT-PCR that silencing of *ENO1* occurred (Supplementary Fig. 5c), we found that silencing of *ENO1* restored expression of *FOXP3* mRNA in iT$_{reg}$-2DG cells (Fig. 6c). Specifically, silencing of *ENO1* in iT$_{reg}$-2DG cells led to the recovery of all *FOXP3* transcripts (fourfold greater abundance than in iT$_{reg}$-2DG cells generated with siRNA-Scr) and an even greater recovery of *FOXP3*-E2 mRNA (13-fold greater abundance than in iT$_{reg}$-2DG cells generated with siRNA-Scr) (Fig. 6c). In addition,

the level of *FOXP3*-E2 mRNA was significantly higher, whereas the level of total *FOXP3* mRNA was slightly lower, in iT$_{reg}$-CTR cells generated in the presence of siRNA-ENO1 than in those generated with siRNA-Scr (Fig. 6c). Together these data established that enolase-1 specifically repressed the expression of *FOXP3*-E2 in iT$_{reg}$ cells.

Properties of CD4$^+$Foxp3-E2$^+$ T cells

To investigate the physiological relevance of our findings reported above, we examined *ex vivo* CD4$^+$Foxp3-E2$^+$ cells and their biological properties. CD4$^+$Foxp3-E2$^+$ cells constituted (on average) 5.94% ± 2.68% of PBMCs from healthy human donors, whereas CD4$^+$ cells expressing total Foxp3 represented 10.20% ± 3.97% of these cells (Supplementary Fig. 6a). Flow cytometry revealed that CD4$^+$Foxp3-E2$^+$ cells had higher expression of T$_{reg}$ cell–associated markers (CD25, CTLA-4, GITR, CD39 and CD71) than did CD4$^+$ cells that expressed total Foxp3 (Supplementary Fig. 6b, c), and they were more proliferative and metabolically active than CD4$^+$ cells that expressed total Foxp3, as indicated by their larger amounts of Ki67 and phosphorylated S6 (Supplementary Fig. 6d). These findings suggested that among all the peripheral human CD4$^+$Foxp3$^+$ T cells, those containing the region encoded by exon 2 represented the fraction with the strongest suppressive properties, in agreement with the results we obtained for iT$_{reg}$ cells.

Defective glycolysis and function of iT$_{reg}$ cells in autoimmunity

We next analyzed the relevance of the findings to human autoimmunity, in patients with RRMS who had not undergone treatment and in patients with T1D. Despite the evidence that the proliferation of T$_{conv}$ cells obtained from subjects with RRMS and stimulated *in vitro* with mAb to CD3 plus mAb to CD28 was similar to that of their counterparts from healthy control subjects (Supplementary Fig. 7a), glycolysis was impaired in T$_{conv}$ cells from subjects with RRMS, as indicated by their diminished basal and maximal glycolysis and glycolytic capacity (Fig. 7a and Supplementary Fig. 7b). iT$_{reg}$ cells generated from T$_{conv}$ cells of subjects with RRMS demonstrated diminished *in vitro* suppressive ability relative to that of those generated from healthy age- and sex-matched control subjects (Fig. 7b). Moreover, iT$_{reg}$ cells from subjects with RRMS had reduced expression of Foxp3-E2, CTLA-4, PD-1 and CD71 and less phosphorylation of S6, and slightly increased expression of GITR, compared with that of iT$_{reg}$ cells from healthy control subjects (Fig. 7c). There was also impaired induction in expression of the 47-kDa and 44-kDa forms of Foxp3 in T$_{conv}$ cells from subjects with RRMS at 24 and 36 h after stimulation with a minimal dose of mAb to CD3 plus mAb to CD28, together with impairment of the IL-2–IL-2R–STAT5 signaling pathway at 24 h (Fig. 7d). We also confirmed the specific decrease in Foxp3-E2 expression in T$_{conv}$ cells from subjects with RRMS, by immunoblot analysis with mAb to Foxp3-E2 (Supplementary Fig. 7c). Of note, we also confirmed those findings in studies of monozygotic twins discordant for RRMS (one twin affected and one twin healthy) who had also not undergone treatment (Fig. 7e), as measured by the induction of Foxp3-E2 in T$_{conv}$ cells stimulated *in vitro* with mAb to CD3 plus mAb to CD28 (Supplementary Fig. 1). Notably, we observed a profound delay in the induction of both the 47- kDa form of Foxp3 and the 44-kDa form of Foxp3 in T$_{conv}$ cells from the twin with RRMS at 24 h, relative to the induction in such cells from the healthy twin (Fig. 7e). At 36 h, the level of the 44- kDa

form of Foxp3 was not significantly lower than its abundance in T_{conv} cells from the healthy twin, whereas the 47-kDa form of Foxp3 was still profoundly lower in abundance (Fig. 7e).

To explore whether altered induction of Foxp3-E2 was a specific feature of RRMS or was instead a common phenomenon in autoimmunity, we also evaluated the induction of Foxp3, T_{reg} cell markers and IL-2–IL-2R–STAT5 signaling in T_{conv} cells obtained from subjects with early-onset T1D and stimulated *in vitro* with mAb to CD3 plus mAb to CD28 (Supplementary Fig. 1). We found that iT_{reg} cells from subjects with T1D had lower expression of Foxp3-E2, CTLA-4, PD-1 and GITR, without differences in the phosphorylation of S6 or expression of CD71, relative to that of iT_{reg} cells from age-matched healthy control subjects, as assessed by flow cytometry (Fig. 8a). At both 24 h and 36 h, there was marked impairment in induction of the 47- and 44- kDa forms of Foxp3 in subjects with T1D relative to their induction in healthy control subjects (Fig. 8b). These phenomena correlated with a significant reduction in the phosphorylation of STAT5 observed at 24 h in T_{conv} cells from subjects with T1D, relative to its phosphorylation in such cells from healthy control subjects (Fig. 8b). We confirmed, by immunoblot analysis with mAb to Foxp3-E2, the specific decrease in Foxp3-E2 (Supplementary Fig. 7d). Of note, we confirmed again the impairment in the induction of Foxp3-E2 in monozygotic twins discordant for T1D. At 24 h, the level of the 47- and 44-kDa forms of Foxp3 in T_{conv} cells from the affected twin was similar to that in cells from the healthy twin, while at 36 h the 47-kDa form was much less abundant in cells from the affected twin than in cells from the healthy twin (Fig. 8c), which confirmed our findings for Foxp3-E2 expression in RRMS, another autoimmune disease. Overall, our data suggested that T_{conv} cells from healthy subjects exhibited normal glycolysis during *in vitro* stimulation with mAb to CD3 plus mAb to CD28, which led to the generation of functional iT_{reg} cells that expressed appropriate amounts of Foxp3-E2 (Supplementary Fig. 8). In subjects with autoimmunity, impaired glycolysis during T_{conv} cell stimulation led to reduced expression of Foxp3-E2 that would account for the diminished regulatory ability of iT_{reg} cells (Supplementary Fig. 8).

Here we found that glycolysis was indispensable for the generation of human iT_{reg} cells from T_{conv} cells through localization of the glycolytic enzyme enolase-1 to the nucleus, which directly affected the induction of specific splicing variants of Foxp3-E2 after enolase-1 bound to the *FOXP3* promoter and CNS2. We confirmed our findings in two different human autoimmune diseases, RRMS and T1D. This emphasizes the link between metabolism and immunotolerance in the development of autoimmunity.

Human iT_{reg} cells can be generated anew from non-regulatory T_{conv} cells, following suboptimal stimulation of the TCR and without the requirement for exogenous regulatory-type cytokines or drugs; this provides evidence that TCR signal strength is a critical determinant of the induction of Foxp3, the generation of T_{reg} cells and the engagement of specific metabolic programs during the activation of T_{conv} cells[11, 17, 18, 19, 31]. In our experimental system, weak (0.1 bead per cell) and short (36-hour) activation of T_{conv} cells via the TCR gave rise to iT_{reg} cells that were the highly proliferative and metabolically active fraction of activated T cells (whose generation closely relies on glycolysis). 2DG (a glycolytic inhibitor) affected the induction of Foxp3, reduced the expression of T_{reg} cell markers and impaired the suppressive function of iT_{reg} cells. The inhibition of FAO via Etx

increased Foxp3 expression and induced iT$_{reg}$ cells with stronger regulatory properties. These results are in agreement with published reports showing that the engagement of distinct metabolic pathways controls the function and differentiation of T cells[17, 18, 19].

Glycolysis fuels the energetic and biosynthetic demands of CD4^{+} T cell growth and proliferation and represents the metabolic program necessary for appropriate cell activation[17, 21, 32]. Compelling experimental evidence suggests that during maximal activation of CD4^{+} T cells, autocrine secretion of IL-2 induces Foxp3 in a small fraction of cells, which leads to conversion into Foxp3^{+} T$_{reg}$ cells, whose stability over time has been questioned[33]. We observed here that weak stimulation of the TCR generated Foxp3^{+} iT$_{reg}$ cells that were stable over time. Therefore, we speculate that the activation of T$_{conv}$ cells induces a self-limiting mechanism of activation through the generation of iT$_{reg}$ cells and thereby induces the maintenance of tolerance. This could help to explain the apparent paradox of the association of T cell immunodeficiency with autoimmunity[34,35]; i.e., a reduced activation rate of T cells (immunodeficiency) might diminish the generation of iT$_{reg}$ cells necessary to replenish the peripheral pool of T$_{reg}$ cells (autoimmunity).

Our study has also demonstrated a crucial role for the glycolytic enzyme enolase-1 and its isoform (i.e., MBP-1) in modulating the expression of specific splicing forms of Foxp3 that were indispensable for the suppressive function of iT$_{reg}$ cells. So far, about twelve different *FOXP3* transcripts have been reported, as well as four to eight different splicing forms of the protein (ranging from 18 kDa to 49 kDa), but their functions are not completely understood[22, 23, 24, 26]. We found that treatment with 2DG was able to diminish the abundance of the Foxp3-E2 splice forms, which we found were necessary for the regulatory function of iT$_{reg}$ cells (as exemplified by the reduced suppressive ability of both iT$_{reg}$-2DG cells and cells generated with siRNA-E2, in which*FOXP3*-E2 was silenced). The splice form that accounted for the suppressive activity of iT$_{reg}$ cells was the 47-kDa form, which contains the region encoded by exon 2. The role of that region has been assessed at a molecular level in various experimental systems[36, 37, 38]. Foxp3 can block the activity of RORγt, a transcription factor associated with the T$_H$17 subset of helper T cells, through direct interaction involving the region encoded by exon 2 (ref. 36). Foxp3 interacts also with the transcription factor RORα, and mutations of sequence in exon 2 encoding the 'LxxLL' motif (where 'x' indicates any amino acid) hamper the interaction and repression by Foxp3 (refs. 37,38). In addition, CD4^{+}CD25^{+} T cells containing spliced forms of *Foxp3* lacking exon 2 are less hypo-responsive and produce more IL-2 than are CD4^{+}CD25^{+} T cells containing the *Foxp3*-E2 splicing form[24].

The recruitment of different factors to *FOXP3* regulatory elements can influence gene expression or alternative splicing through a combination of physical mechanisms ranging from direct interaction to transient chromatin modification. Among those factors, MBP-1, which is derived from alternative translation of *ENO1* transcripts, has been reported to bind DNA and to suppress gene expression[27, 28, 29, 30]. We found that under conditions of inhibition of glycolysis (treatment with 2DG), there was an increase in enolase-1 on both the *FOXP3* promoter and *FOXP3* CNS2, and this was associated with reduced expression of total *FOXP3* and the *FOXP3*-E2 splicing variant. In addition, when glycolysis was inhibited (in iT$_{reg}$-2DG cells) during RNA-mediated interference of*ENO1*, the observed recovery of

total Foxp3 and the Foxp3-E2 isoform depended on the non-glycolytic activity of enolase-1. In contrast, silencing of *ENO1* in the absence of treatment with 2DG (in iT_{reg}-CTR cells) lead to a reduction in Foxp3 expression that could be ascribed to impairment of the glycolytic activity of enolase-1. Our data have identified a previously unknown molecular mechanism that links a specific glycolytic enzyme to the regulation of a 'master gene' (*FOXP3*) whose product is necessary for the induction and function of T_{reg} cells. In resting T_{conv} cells, with low glycolytic demands, enolase-1 was specifically recruited to *FOXP3* regulatory regions, and this correlated with no Foxp3 expression. Activation of the TCR led to an increase in glucose uptake and glycolysis, which supported the energetic needs of T_{conv} cells and drove appropriate Foxp3 expression; impairment of the glycolytic pathway (with 2DG) during the activation of T_{conv} cells hampered the induction of Foxp3-E2 after accumulation of the enolase-1 isoforms in the nucleus on *FOXP3* regulatory regions. This indicated that glycolysis was required for the generation of iT_{reg} cells following the activation of T_{conv} cells. We also found that iT_{reg}-2DG cells had an impairment in the IL-2– IL-2R–STAT5 signaling pathway (which has a pivotal role in the induction of Foxp3 and the generation and homeostasis of T_{reg} cells)[25, 39], whereas iT_{reg}-Etx cells exhibited more activation of this pathway. In T_{conv} cells, a major consequence of IL-2 signaling is the phosphorylation of STAT5, which binds to the *FOXP3* promoter; this leads to *FOXP3* expression and the acquisition of suppressive ability by the cells[40, 41]. This is a key event in the generation of T_{reg} cells, as shown by the fact that STAT5- or IL-2Rγ-deficient mice have considerably fewer Foxp3+ T_{reg} cells than their wild-type counterparts have[42]. We applied those findings to two human autoimmune diseases, including studies of disease-discordant monozygotic twins, in which a reduced suppressive function of iT_{reg} cells was associated specifically with impaired expression of Foxp3-E2, secondary to a glycolytic defect during the activation of T_{conv} cells. In summary, our data suggest that distinct metabolic pathways contribute to the generation of 'waves' of T_{reg} cells during T cell activation to replenish the peripheral T_{reg} cell pool and protect from loss of immunotolerance[34, 35]. Targeted manipulation of metabolic disturbances could be instrumental in modulating immunotolerance in autoimmunity.

Methods

Subjects and iT$_{reg}$ cell induction

iT_{reg} cells were induced from CD4+CD25− cells (T_{conv} cells) from healthy donors and subjects with RR-MS or T1D. The study was approved by the Institutional Review Board of the Università degli Studi di Napoli "Federico II", and peripheral blood was obtained from subjects with RR-MS and healthy control subjects after they signed a written informed consent approved by the Institutional Review Board. Subjects with RR-MS (including two pairs of disease-discordant monozygotic twins) had all not undergone treatment and were 40 ± 20 years of age (at a female/male ratio of 4:1), with relapsing-remitting disease and with a Kurtzke expanded disability status score between 0 and 4 (ref. 43). Healthy donors were matched for age, body mass index and sex with the subjects with RR-MS and had no history of inflammatory, endocrine or autoimmune disease. All blood samples from patients and controls were collected at 9:00 a.m. into heparinized Vacutainers (BD Biosciences) and were processed within the following 4 h.

Subjects with T1D (8 ± 3 years age, at a female/male ratio of 1:1), including the pairs of disease-discordant monozygotic twins, were recruited after resolution of diabetic ketoacidosis, with blood glucose values between 80 mg/dl and 180 mg/dl, after glycemic stabilization through the use of exogenous insulin, achieved in 5 d. Diabetes was defined according to the Global International Diabetes Federation/International Society for Pediatric and Adolescent Diabetes Guidelines for Diabetes in Childhood and Adolescence[44] and included symptoms of diabetes, in addition to a random plasma glucose concentration of 11.1 mmol/l (200 mg/dl) or a fasting plasma glucose concentration of 7.0 mmol/l (126 mg/dl), or a glucose concentration of 11.1 mmol/l (200 mg/dl) 2 h after glucose loading during an oral glucose-tolerance test, and a glycated hemoglobin (HbA_{1c}) of 6.5 (ref. 44). The following criteria were used for the selection of healthy control subjects for studies of T1D: a fasting blood glucose concentration of <5.5 mmol/l (<100 mg/dl), negative personal and familial history of autoimmune disorders, and negativity for islet autoantibodies at the 99th percentile. The children with T1D and control subjects (matched for age, sex and body mass index) were recruited at the Sezione di Pediatria, Dipartimento di Scienze Mediche Traslazionali, Università di Napoli "Federico II", after the Institutional Review Board of the Università degli Studi di Napoli "Federico II" approved the study and parents provided their written informed consent.

For the generation of iT_{reg} cells, after Ficoll hypaque–gradient centrifugation (GE-Healthcare), T_{conv} cells were isolated from PBMCs by negative selection with a human $CD4^+CD25^+$ T cell kit (Invitrogen) (cell purity >98% by flow cytometry), and cells were cultured (2×10^6 cells per ml) in six-well plates (Becton-Dickinson; Falcon) with RPMI-1640 medium supplemented with 100 UI/ml penicillin, 100 μg/ml streptomycin (Life Technologies) and either 5% autologous serum or 5% AB human serum (Invitrogen). Cells were stimulated for 36 h with Dynabeads coated with mAb to CD3 plus mAb to CD28 (Invitrogen) at a density of 0.1 bead per cell. T_{conv} cells were then stained with the following mAbs: fluorescein isothiocyanate (FITC)-conjugated anti–human CD4 (RPA-T4; 555346BD; PharMingen), phycoerythrin (PE)–indodicarbocyanine (Cy5)–conjugated anti–human CD25 (M-A251; 555433; BD PharMingen). Cells were sorted by flow cytometry on the basis of their cell-surface expression of CD25 with a MoFlo high-performance cell sorter (Dako/Beckman-Coulter) or a BD FACSJazz (Becton-Dickinson) (Supplementary Fig. 1). For the generation of iT_{reg} cells in the presence of inhibitors of specific metabolic pathways, T_{conv} cells were stimulated for 36 h with Dynabeads coated with mAb to CD3 plus mAb to CD28 (0.1 bead per cell) (Invitrogen) in the absence or presence of 1 mM 2-deoxy-D-glucose (2DG) (Sigma-Aldrich) or 200 μM etomoxir (Etx) (Sigma-Aldrich). Cells obtained from each culture were then stained with FITC-conjugated anti–human CD4 (RPA-T4; 555346; BD PharMingen) and PE-Cy5–conjugated anti–human CD25 (M-A251; 555433; BD PharMingen), and iT_{reg} cells from each experimental culture were then sorted by flow cytometry (cell purity >98% by flow cytometry) (Supplementary Fig. 3). Cells at 36 h after sorting by flow cytometry are called 'iT_{reg}-CTR cells', 'iT_{reg}-2DG cells', 'iT_{reg}-Etx cells' and 'T_{conv} cells' here.

Molecular signaling and immunoblot analysis

iT$_{reg}$-CTR, iT$_{reg}$-2DG and iT$_{reg}$-Etx cells sorted by flow cytometry were lysed after 1 h of culture with or without stimulation with Dynabeads coated with mAb to CD3 plus mAb to CD28 (0.2 bead per cell) (Invitrogen). T$_{conv}$ cells from subjects with RR-MS or T1D and healthy subjects were lysed 24 and 36 h after stimulation with Dynabeads coated with mAb to CD3 plus mAb to CD28 (0.1 bead per cell) (Invitrogen). Subcellular fractionations were performed with a nuclear-cytosol fractionation kit (NE-PER Nuclear and Cytoplasmic Extraction Reagents; Thermo-Fisher). Total cell lysates were obtained incubation of cells for 20 min at 4 °C in a solution of 50 mM Tris-HCl (pH 7.5), 150 mM NaCl and 1.0% Triton X-100, plus SigmaFast protease inhibitor (S8820; Sigma-Aldrich) and Sigma phosphatase inhibitor (P5726; Sigma-Aldrich), and immunoblot analyses were performed as described[45]. The following mAbs used were used for normalization of nuclear extracts: antibody to S6 phosphorylated at Ser240 and Ser244 (2215), anti-S6 (5G10, 2217), anti-enolase-1 (3810), antibody to STAT3 phosphorylated at Tyr705 (3E2; 9138), anti-STAT3 (79D7; 4904), antibody to STAT5 phosphorylated at Tyr694 (9351), anti-STAT5 (9352) (all 1:1,000 dilution; all from Cell Signaling Technology); anti-Erk1/2 (H72, SC292838) (Santa Cruz Biotechnology); antibody to all Foxp3 (PCH101; 12-4776), antibody to Foxp3-E2 (150D/E4; 14-4774) (all 1:500 dilution; all from eBioscience); anti-enolase-1 (1:500 dilution; H-300; SC15343) and anti-MCM7 (1:3,000 dilution; 141.2; SC9966) (all from Santa Cruz Biotechnology). All filters were quantified by densitometry as described[45]. Results were calculated as the densitometry of each phosphorylated protein normalized to that of its total form (S6, STAT3 and STAT5) or normalized to that of Erk1/2 (enolase-1 and Foxp3) or MCM7 (enolase-1 from nuclear extracts) and are presented relative to results obtained for control samples.

'Seahorse' experiments

Metabolic profiles of T$_{conv}$ and iT$_{reg}$ cells were evaluated in the presence or absence of stimulation with Dynabeads coated with mAb to CD3 plus mAb to CD28 (0.1 bead per cell) (Invitrogen). Real-time measurements of oxygen consumption rate (OCR) and extracellular acidification rate (ECAR) were made with an XF-96 Extracellular Flux Analyzer (Seahorse Bioscience). T$_{conv}$ cells and iT$_{reg}$ cells were plated in XF-96 plates (Seahorse Bioscience) at a density of 2×10^5 cells per well and were cultured with RPMI-1640 medium supplemented with 5% AB human serum. OCR was measured in XF medium (non-buffered DMEM medium containing 10 mM glucose, 2 mM L-glutamine and 1 mM sodium pyruvate) under basal conditions and in response to 5 μM oligomycin, 1.5 μM of FCCP (carbonylcyanide-4-(trifluoromethoxy)-phenylhydrazone) and 1 μM of antimycin and rotenone (Sigma-Aldrich). ECAR was measured in XF medium in basal conditions and in response to 10 mM glucose, 5 μM oligomycin and 100 mM of 2DG (all from Sigma-Aldrich). Experiments with the Seahorse system were done with the following assay conditions: 3 min of mixture; 3 min of waiting; and 3 min of measurement. For the analysis of FAO, the XF Palmitate-BSA FAO substrate was used (Seahorse Bioscience). FAO was measured in FAO buffer containing 111 mM NaCl, 4.7 mM KCl, 2 mM MgSO$_4$ and 1.2 mM Na$_2$HPO$_4$, supplemented with 2.5 mM glucose, 0.5 mM carnitine and 5 mM HEPES, pH7.4 (all from Sigma-Aldrich) Etomoxir (final concentration, 40 μM; Sigma-Aldrich) was added 15 min before the 'XF' assay (time 0). At time 0, cells were given 30 μl of 1 mM palmitate

conjugated to 0.17 mM BSA. FAO was calculated as the ratio of the FCCP-stimulated OCR in the presence of palmitate to the FCCP-stimulated OCR in the presence of Etx.

Flow cytometry, T cell proliferation and CFSE staining

For staining of PBMCs, T_{conv} or iT_{reg} cells, the following mAbs were used: FITC-conjugated anti–human CD4 (RPA-T4; 555346; BD PharMingen), PE-conjugated anti–human CD25 (M-A251; 555432; BD PharMingen), PE-Cy5-conjugated anti–human CD25 (M-A251; 555433; BD PharMingen), allophycocyanin (APC)-conjugated anti–human CD39 (TU66; 560239; BD PharMingen), APC-conjugated anti–human CD71 (M-A712; 551374; BD PharMingen), APC-conjugated anti–human CD127 (HIL-7R-M21; 555598; BD PharMingen), PE-Cy5-conjugated anti–human CD152 (BNI3 555854; BD PharMingen), PE-conjugated anti–human GITR (DT5D3; 130-092-895; Miltenyi Biotec), PE-Cy5-conjugated anti–human CD45RO (UCHL1 MCA461C; Serotec), FITC-conjugated anti–human CCR7 (150503; FAB197F; R&D Systems), APC-conjugated anti–human CD62L (DREG-56 559772; BD Pharmingen) and peridinin chlorophyll protein (PerCP)–cyanine 5.5 (Cy5.5)–conjugated anti–human CD279 (PD-1; EH12.1 581273; BD Pharmingen). Thereafter cells were washed, fixed and permeabilized (fixation-permeabilization buffer; eBioscience) and were stained with the following mAbs: PE–anti-Foxp3 (PCH101; 12-4776; eBioscience), PE–anti-Foxp3 (150D/E4; 12-4774; eBioscience), Alexa Fluor 647–conjugated antibody to ribosomal protein S6 phosphorylated at Ser235 and Ser236 (D57.2.2E; 4803S; Cell Signaling) and FITC–anti-Ki67 (B56; 556026 BD Biosciences). Analyses were performed with Diva software (BD) and FlowJo software (Tree Star). For T cell–proliferation assays, purified T cells (5×10^4 cells per well) were cultured as described[26]. The fluorescent dye CFSE (5,6-carboxyfluorescein diacetate succinimidyl ester) was used at a concentration of 1 μg/ml (Invitrogen). Flow cytometry analyzing CFSE dilution was performed by gating on CD4$^+$CFSE$^+$cells stimulated for 96 h with Dynabeads coated with mAb to CD3 plus mAb to CD28 (0.2 bead per cell) (Invitrogen) alone or cultured with iT_{reg} cells at varous ratios (from 1:1 to 8:1, CD4$^+$ T cells/iT_{reg} cells) in round-bottomed 96-well plates for cell-cell contact experiments or in 24-well plates for Transwell experiments (all from Becton-Dickinson).

RNA extraction, qRT-PCR, qPCR and siRNA

Total RNA was extracted with Triazol (Invitrogen). cDNA was synthesized in a 20-μl reaction volume containing 1 μg of total RNA, 100 units of Superscript III Reverse Transcriptase (Invitrogen) and 1 μl of random primers (200 ng/μl). mRNA was reverse-transcribed for 1 h at 50 °C, and the reaction was heat-inactivated for 15 min at 70 °C. The products were stored at −20 °C until use. Quantitative RT-PCR and quantitative PCR were performed on a 7500 RT-PCR System (Applied Biosystems) with a SYBR Green detection system (FS Universal SYBR Green MasterRox; Roche Applied Science). The *FOXP3* splice variants primers used are in Supplementary Table 1. Primers for 18S were used as internal standard control for the reactions (Supplementary Table 1).

For knockdown of *FOXP3* and *ENO1* with siRNA, cells were transiently transfected, with a Neon Transfection System, with siRNA at a final concentration of 10 nM (in medium without serum), and incubation was continued for 48 h. RNA with a scrambled sequence, at

the same concentration, was used as negative control. siRNA was designed to target *FOXP3* exon 5 (target sequence, 5′-UCGAAGAGCCAGAGGACUU-3′ or exon 2 (target sequence, 5′-GGCCACAUUUCAUGCACCA-3′) or with a scrambled sequence (target sequence, 5′-AUUGAGUGUAGAUUAAGUA-3′). A mixture of siRNA specific for all *ENO1* isoforms was used (target sequences, 5′-CAGUGGUGUCUAUCGAAGA-3′ and 5′-CCGUGACCGAGUCUCUUCA-3′) (4390821; Life Technologies). T_{conv} cells were transfected under the following conditions: pulse voltage, 2,400 V; pulse width, 20 ms; pulse number, 1. Then, cells were stimulated with Dynabeads coated with mAb to CD3 plus mAb to CD28 (0.1 beads/cell) (Invitrogen). After 36 h of stimulation, immunoblot analysis or RT-PCR was performed for confirmation of specific silencing.

Chromatin immunoprecipitation

After the appropriate treatment, cells ($\sim 7 \times 10^5$ for each antibody) were fixed for 10 min at room temperature by the addition of 1 volume of 2% formaldehyde to a final concentration of 1%; the reaction was quenched by the addition of glycine to a final concentration of 125 mM. Fixed cells were harvested and the pellet was resuspended in 1 ml of lysis buffer (10 mM Tris-HCl, pH 8.0, 10 mM NaCl and 0.2% NP-40) containing 1× protease inhibitor cocktail (Roche Applied Science). The lysates were sonicated to produce DNA fragments 300–600 base pairs in length. Sonicated samples were centrifuged and supernatants were diluted twofold in chromatin immunoprecipitation buffer (20 mM Tris-HCl, pH 8.0, 150 mM NaCl, 2 mM EDTA and 1% Triton X-100). An aliquot (1/10) of sheared chromatin was further treated with proteinase K, then underwent extraction with phenol-chloroform and precipitation for measurement of DNA concentration and shearing efficiency (input DNA). Chromatin-immunoprecipitation reactions were set up according to the manufacturer's instructions (Abcam). The sheared chromatin was precleared by incubation for 2 h with 1 µg of non-immune mouse IgG (sc-2025) and rabbit IgG (sc-2027) (both from Santa Cruz Biotechnology) and 20 µl of Protein A/G PLUS-Agarose (Santa Cruz Biotechnology) saturated with salmon sperm (1 mg/ml). Precleared chromatin was divided in aliquots and then was incubated for 16 h at 4 °C with 1 µg of specific antibody (anti-enolase-1: 3810 (Cell Signaling Technology) or sc-15343 (Santa Cruz Biotechnology)) and non-immune IgG (identified above). The immunocomplexes were recovered by incubation for 3 h at 4 °C with 20 µl of protein-A/G agarose, then beads were washed with wash buffers according to the manufacturer's instructions (sc-2003; Santa Cruz Biotechnology), and immunoprecipitated DNA was recovered and analyzed by quantitative PCR (primers, Supplementary Table 1).

Methylation experiments

Methyl-sensitive PCR was used for analysis of the methylation status of the CpG island near the CNS2 region of *FOXP3*. Genomic DNA was prepared as described[46]. Genomic DNA (1 µg) isolated from cells was digested overnight at 37 °C with 10 U of HpaII or MspI. Two neighboring regions of the *FOXP3* CpG island have been analyzed by real-time PCR with specific primers (Supplementary Table 1). H19 and UEB2B were used as a control for fully methylated and unmethylated regions (primers, Supplementary Table 1).

Author Manuscript

Statistical analysis

All statistical analyses were performed with SPSS software, version 16 for Mac (SPSS), and the GraphPad program (Abacus Concepts). All the comparisons for immunoblot, PCR, proliferation and 'Seahorse' analyses were evaluated with the nonparametric Wilcoxon/ Kruskal-Wallis or the paired two-tailed Student's *t*-test. For all analyses, we used two-sided tests, with a *P* value of <0.05 indicative of statistical significance.

Supplementary Material

Refer to Web version on PubMed Central for supplementary material.

Acknowledgments

References

1. Ohkura N, Kitagawa Y, Sakaguchi S. Development and maintenance of regulatory T cells. Immunity. 2013; 38:414–423. [PubMed: 23521883]

2. Gavin MA, et al. Foxp3-dependent programme of regulatory T-cell differentiation. Nature. 2007; 445:771–775. [PubMed: 17220874]

3. Lin W, et al. Regulatory T cell development in the absence of functional Foxp3. Nat Immunol. 2007; 8:359–368. [PubMed: 17273171]

4. Bilate AM, Lafaille JJ. Induced CD4+Foxp3+ regulatory T cells in immune tolerance. Annu Rev Immunol. 2012; 30:733–758. [PubMed: 22224762]

5. Goldstein JD, et al. Role of cytokines in thymus- versus peripherally derived-regulatory T cell differentiation and function. Front Immunol. 2013; 4:155. [PubMed: 23801992]

6. Chen W, et al. Conversion of peripheral CD4+CD25− naive T cells to CD4+CD25+ regulatory T cells by TGF-β induction of transcription factor Foxp3. J Exp Med. 2003; 198:1875–1886. [PubMed: 14676299]

7. Zheng SG, Gray JD, Ohtsuka K, Yamagiwa S, Horwitz DA. Generation ex vivo of TGF- β-producing regulatory T cells from CD4+CD25− precursors. J Immunol. 2002; 169:4183–4189. [PubMed: 12370347]

8. Walker MR, et al. Induction of FoxP3 and acquisition of T regulatory activity by stimulated human CD4+CD25− T cells. J Clin Invest. 2003; 112:1437–1443. [PubMed: 14597769]

9. Walker MR, Carson BD, Nepom GT, Ziegler SF, Buckner JH. De novo generation of antigen-specific CD4+CD25+ regulatory T cells from human CD4+CD25− cells. Proc Natl Acad Sci USA. 2005; 102:4103–4108. [PubMed: 15753318]

10. Curotto de Lafaille MA, Lino AC, Kutchukhidze N, Lafaille JJ. CD25− T cells generate CD25+Foxp3+ regulatory T cells by peripheral expansion. J Immunol. 2004; 173:7259–7268. [PubMed: 15585848]

11. Miskov-Zivanov N, Turner MS, Kane LP, Morel PA, Faeder JR. The duration of T cell stimulation is a critical determinant of cell fate and plasticity. Sci Signal. 2013; 6:ra97. [PubMed: 24194584]

12. Van Panhuys N, Klauschen F, Germain RN. T-cell-receptor-dependent signal intensity dominantly controls CD4^{+} T cell polarization in vivo. Immunity. 2014; 41:63–74. [PubMed: 24981853]

13. Turner MS, Kane LP, Morel PA. Dominant role of antigen dose in CD4^{+}Foxp3^{+}regulatory T cell induction and expansion. J Immunol. 2009; 183:4895–4903. [PubMed: 19801514]

14. Haxhinasto S, Mathis D, Benoist C. The AKT-mTOR axis regulates de novo differentiation of CD4^{+}Foxp3^{+} cells. J Exp Med. 2008; 205:565–574. [PubMed: 18283119]

15. Sauer S, et al. T cell receptor signaling controls Foxp3 expression via PI3K, Akt, and mTOR. Proc Natl Acad Sci USA. 2008; 105:7797–7802. [PubMed: 18509048]

16. Liang S, et al. Conversion of CD4^{+}CD25^{−} cells into CD4^{+}CD25^{+} regulatory T cells in vivo requires B7 costimulation, but not the thymus. J Exp Med. 2005; 201:127–137. [PubMed: 15630140]

17. Michalek RD, et al. Cutting edge: distinct glycolytic and lipid oxidative metabolic programs are essential for effector and regulatory CD4^{+} T cell subsets. J Immunol. 2011; 186:3299–3303. [PubMed: 21317389]

18. Procaccini C, et al. An oscillatory switch in mTOR kinase activity sets regulatory T cell responsiveness. Immunity. 2010; 33:929–941. [PubMed: 21145759]

19. Pearce EL, Pearce EJ. Metabolic pathways in immune cell activation and quiescence. Immunity. 2013; 38:633–643. [PubMed: 23601682]

20. Gerriets VA, et al. Metabolic programming and PDHK1 control CD4^{+} T cell subsets and inflammation. J Clin Invest. 2015; 125:194–207. [PubMed: 25437876]

21. Chang CH, et al. Posttranscriptional control of T cell effector function by aerobic glycolysis. Cell. 2013; 153:1239–1251. [PubMed: 23746840]

22. Kaur G, Goodall JC, Jarvis LB, Hill Gaston JS. Characterization of Foxp3 splice variants in human CD4^{+} and CD8^{+} T cells–identification of Foxp3 7 in human regulatory T cells. Mol Immunol. 2010; 48:321–332. [PubMed: 20688398]

23. Smith EL, Finney HM, Nesbitt AM, Ramsdell F, Robinson MK. Splice variants of human FOXP3 are functional inhibitors of human CD4^{+} T-cell activation. Immunology. 2006; 119:203–211. [PubMed: 17005002]

24. Allan SE, et al. The role of 2 FOXP3 isoforms in the generation of human CD4^{+} Tregs. J Clin Invest. 2005; 115:3276–3284. [PubMed: 16211090]

25. Cheng G, Yu A, Malek TR. T-cell tolerance and the multi-functional role of IL-2R signaling in T-regulatory cells. Immunol Rev. 2011; 241:63–76. [PubMed: 21488890]

26. Carbone F, et al. Regulatory T cell proliferative potential is impaired in human autoimmune disease. Nat Med. 2014; 20:69–74. [PubMed: 24317118]

27. Wang W, et al. Identification of alpha-enolase as a nuclear DNA-binding protein in the zona fasciculata but not the zona reticularis of the human adrenal cortex. J Endocrinol. 2005; 184:85–94. [PubMed: 15642786]

28. Hsu KW, et al. The activated Notch1 receptor cooperates with α-enolase and MBP-1 in modulating c-myc activity. Mol Cell Biol. 2008; 28:4829–4842. [PubMed: 18490439]

29. Subramanian A, Miller DM. Structural analysis of alpha-enolase. Mapping the functional domains involved in down-regulation of the c-myc protooncogene. J Biol Chem. 2000; 275:5958–5965. [PubMed: 10681589]

30. Pancholi V. Multifunctional alpha-enolase: its role in diseases. Cell Mol Life Sci. 2001; 58:902–920. [PubMed: 11497239]

31. Gottschalk RA, Corse E, Allison JP. TCR ligand density and affinity determine peripheral induction of Foxp3 in vivo. J Exp Med. 2010; 207:1701–1711. [PubMed: 20660617]

32. Macintyre AN, et al. The glucose transporter Glut1 is selectively essential for CD4 T cell activation and effector function. Cell Metab. 2014; 20:61–72. [PubMed: 24930970]

33. Malek TR, Castro I. Interleukin-2 receptor signaling: at the Interface between tolerance and immunity. Immunity. 2010; 33:153–165. [PubMed: 20732639]

34. Carneiro-Sampaio M, Coutinho A. Early-onset autoimmune disease as a manifestation of primary immunodeficiency. Front Immunol. 2015; 6:185. [PubMed: 25999944]

35. King C, Ilic A, Koelsch K, Sarvetnick N. Homeostatic expansion of T cells during immune insufficiency generates autoimmunity. Cell. 2004; 117:265–277. [PubMed: 15084263]

36. Zhou L, et al. TGF-β-induced Foxp3 inhibits T_H17 cell differentiation by antagonizing RORγt function. Nature. 2008; 453:236–240. [PubMed: 18368049]

37. Du J, Huang C, Zhou B, Ziegler SF. Isoform-specific inhibition of RORα-mediated transcriptional activation by human FOXP3. J Immunol. 2008; 180:4785–4792. [PubMed: 18354202]

38. Magg T, Mannert J, Ellwart JW, Schmid I, Albert MH. Subcellular localization of FOXP3 in human regulatory and nonregulatory T cells. Eur J Immunol. 2012; 42:1627–1638. [PubMed: 22678915]

39. Maruyama T, Konkel JE, Zamarron BF, Chen W. The molecular mechanisms of Foxp3 gene regulation. Semin Immunol. 2011; 23:418–423. [PubMed: 21752667]

40. D'Cruz LM, Klein L. Development and function of agonist-induced CD25^{+}Foxp3^{+}regulatory T cells in the absence of interleukin 2 signaling. Nat Immunol. 2005; 6:1152–1159. [PubMed: 16227983]

41. Passerini L, et al. STAT5-signaling cytokines regulate the expression of FOXP3 in CD4^{+}CD25^{+} regulatory T cells and CD4^{+}CD25^{−} effector T cells. Int Immunol. 2008; 20:421–431. [PubMed: 18270368]

42. Fontenot JD, Rasmussen JP, Gavin MA, Rudensky AY. A function for interleukin 2 in Foxp3-expressing regulatory T cells. Nat Immunol. 2005; 6:1142–1151. [PubMed: 16227984]

43. Kurtzke JF. Rating neurologic impairment in multiple sclerosis: an expanded disability status scale (EDSS). Neurology. 1983; 33:1444–1452. [PubMed: 6685237]

44. Craig ME, Hattersley A, Donaghue KC. Definition, epidemiology and classification of diabetes in children and adolescents. Pediatr Diabetes. 2009; 10:3–12. [PubMed: 19754613]

45. De Rosa V, et al. A key role of leptin in the control of regulatory T cell proliferation. Immunity. 2007; 26:241–255. [PubMed: 17307705]

46. Cuozzo C, et al. DNA damage, homology-directed repair, and DNA methylation. Plos Genet. 2007; 3:e110. [PubMed: 17616978]
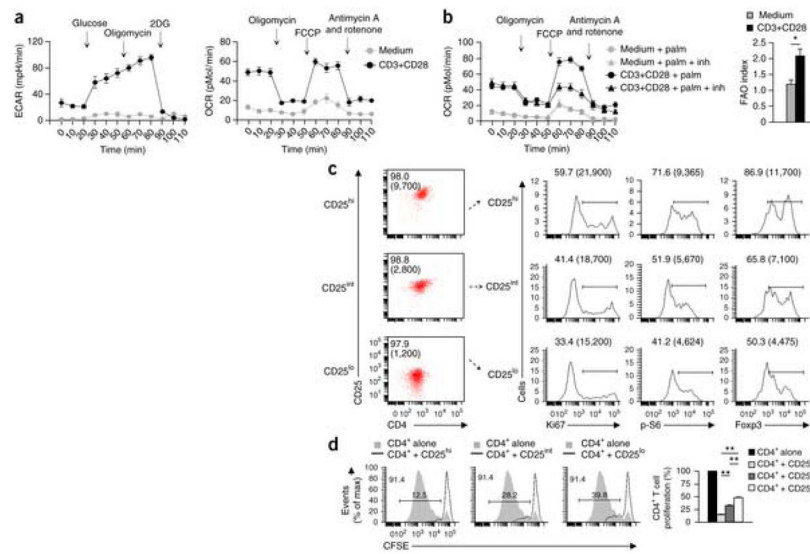
Figure 1.

Generation of human iT$_{reg}$ cells from T$_{conv}$ cells during weak stimulation of the TCR. (**a**) ECAR, as an indicator of glycolysis (left), and OCR, quantifying mitochondrial respiration (right), of T$_{conv}$ cells after 24 h *in vitro* stimulation with medium alone or with mAb to CD3 plus mAb to CD28 (CD3+CD28) (key), in the presence of (above plots) glucose, the ATP-synthase inhibitor oligomycin and 2DG (left), or oligomycin, the uncoupling reagent FCCP and the respiratory-chain inhibitors antimycin A plus rotenone (right), administered sequentially (dotted downward arrows). (**b**) OCR, quantifying FAO (left), of T$_{conv}$ cells stimulated for 24 h *in vitro* as in **a**, right, in the presence of the specific FAO substrate palmitate alone (+ palm) or palmitate plus the FAO inhibitor Etx (+ palm + inh), and their FAO index (right), calculated as ratio of the FCCP-stimulated OCR in the presence of palmitate to the FCCP-stimulated OCR in the presence of palmitate plus inhibitor. (**c**) Flow cytometry of CD4$^+$CD25$^+$ T cells sorted by flow cytometry on the basis of surface CD25 expression (far left), and expression of Ki67, phosphorylation of S6 and expression of Foxp3 (right) in CD25^{hi}, CD25^{int} and CD25^{lo} cells gated as at left. Numbers in plots indicate percent CD25^{hi} cells (top), CD25^{int} cells (middle) or CD25^{lo} cells (bottom) or mean fluorescence intensity (MFI) (in parentheses) of CD25 in those cells (far left), or percent Ki67$^+$ cells (left), cells with phosphorylated S6 (middle) or Foxp3$^+$ cells (right), as well as the MFI (in parentheses) of Ki67 (left), phosphorylated (p-) S6 (middle) or Foxp3 (right). (**d**) Proliferation (left) of CFSE-labeled CD4$^+$ T cells stimulated for 96 h *in vitro* with mAb to CD3 plus mAb to CD28 and cultured alone (CD4$^+$ alone) or in the presence of flow cytometry–sorted CD25^{hi}, CD25^{int} or CD25^{lo} T cells (above plots), and % proliferation of CD4$^+$ T cells in those conditions (far right). Numbers in plots (left) indicate percent CFSE dilution in CD4$^+$ T cells cultured alone (top left); numbers above bracketed lines indicate % CFSE dilution in CD4$^+$ T cells cultured with iT$_{reg}$ cells. *$P < 0.05$ and **$P < 0.0001$ (paired two-tailed Student's *t*-test (**b**) or Wilcoxon matched-pairs test (**d**)). Data are from one experiment representative of 2 with technical duplicates (**a**; mean ± s.e.m.), 3 experiments with technical duplicates (**b**; mean ± s.e.m. (left) or mean ± s.e.m. of $n = 18$ (right)), one experiment representative of 8 (**c**), one experiment representative of 3 (**d**, left) or 3
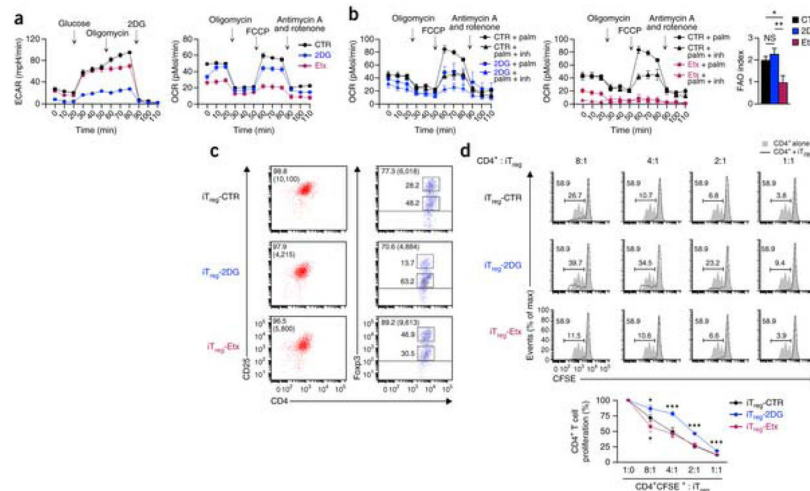
independent experiments with technical triplicates (**d**, right; mean ± s.e.m. of $n = 9$ replicates).

Figure 2.
Generation of human iT$_{reg}$ cells from T$_{conv}$ cells during weak stimulation of the TCR in the presence of inhibitors of either glycolysis or FAO. (**a**) ECAR (left) and OCR (right) of T$_{conv}$ cells stimulated for 24 h *in vitro* with mAb to CD3 plus mAb to CD28 (in conditions as in Fig. 1a; above plots), grown in the absence (control (CTR)) or in the presence of 2DG or Etx (key) (as in Supplementary Fig. 3). (**b**) OCR, quantifying FAO, of T$_{conv}$ cells stimulated for 24 h *in vitro* with mAb to CD3 plus mAb to CD28 (in conditions as in **a**, right; above plots), grown in the absence of 2DG or Etx (control (CTR)) or in the presence of 2DG (left) or Etx (middle), and in the presence of palmitate alone or palmitate plus inhibitor (as in Fig. 1b), and the FAO index of those cells (right; calculated as in Fig. 1b). (**c**) Flow cytometry analyzing the expression of CD25 and CD4 (left), and of Foxp3 and CD4 (right), by CD4$^+$CD25^{hi} iT$_{reg}$-CTR, iT$_{reg}$-2DG and iT$_{reg}$-Etx cells sorted by flow cytometry. Numbers in plots (top left corner) indicate percent CD25$^+$ cells or MFI (in parentheses) of CD25 (left) or percent Foxp3$^+$+ cells or MFI (in parentheses) of Foxp3 (right); numbers adjacent to outlined areas (right) indicate percent Foxp3^{hi} cells (top) or Foxp3^{int} cells (bottom). (**d**) Proliferation of CFSE-labeled CD4$^+$ T cells stimulated for 96 h *in vitro* with mAb to CD3 plus mAb to CD28 and cultured alone (filled gray curves) or in the presence of iT$_{reg}$-CTR, iT$_{reg}$-2DG or iT$_{reg}$-Etx cells (black lines) at various ratios (CFSE$^+$CD4$^+$ T cells to iT$_{reg}$ cells, 8:1 to 1:1; above plots). Numbers in plots indicate percent CFSE dilution in CD4$^+$ T cells cultured alone (top left); numbers above bracketed lines indicate percent CFSE dilution in CD4$^+$ T cells cultured with iT$_{reg}$ cells. Below, frequency of proliferation of CD4$^+$T cells in the conditions above ('–' indicates CD4$^+$ T cells alone). NS, not significant ($P > 0.05$); *$P < 0.05$, **$P < 0.001$ and ***$P < 0.0001$, iT$_{reg}$-2DG versus iT$_{reg}$-CTR or iT$_{reg}$-Etx versus iT$_{reg}$-CTR in **d** (paired two-tailed Student's *t*-test (**b**) or Wilcoxon matched-pairs test (**d**)). Data are from one experiment representative of two experiments with technical duplicates (**a**; mean ± s.e.m.), three independent experiments with technical duplicates (**b**; mean ± s.e.m. (left) or mean ± s.e.m. of $n = 18$ (right)), one experiment representative of eight experiments (**c**), one experiment representative of three (**d**, top), or three independent experiments with technical triplicates (**d**, bottom; mean ± s.e.m. of $n = 45$ (1:1 ratio, iT$_{reg}$-CTR cells from five subjects), $n = 36$ (1:1 ratio, iT$_{reg}$-2DG cells from four subjects), $n = 27$
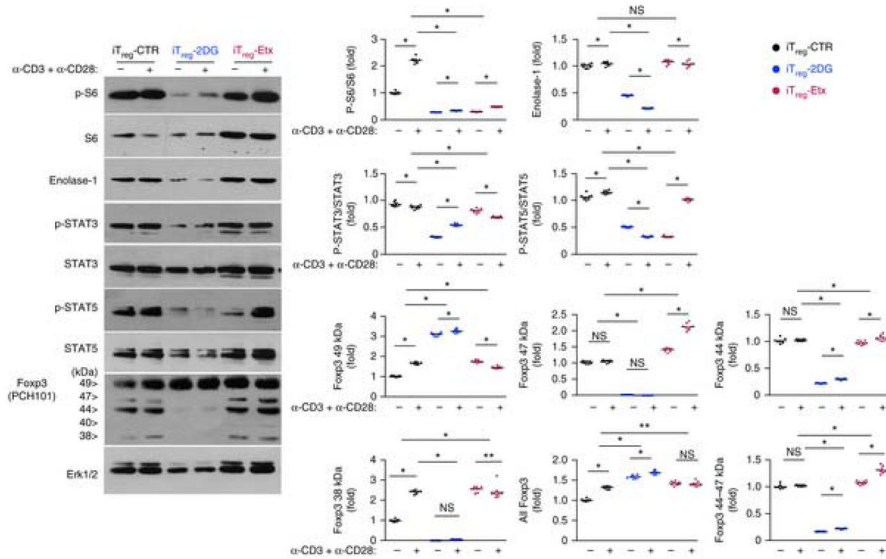
(1:1 ratio, iT$_{reg}$-Etx cells from three subjects), or $n = 18$ (all other conditions, cells from two subjects).
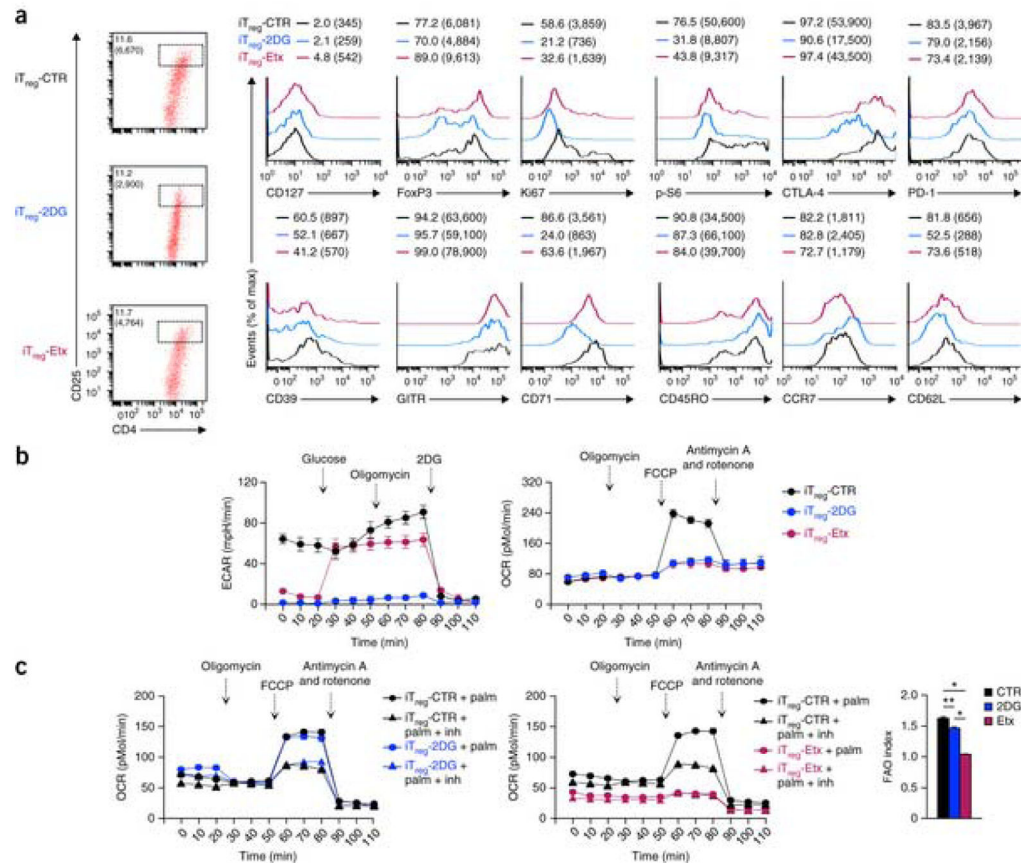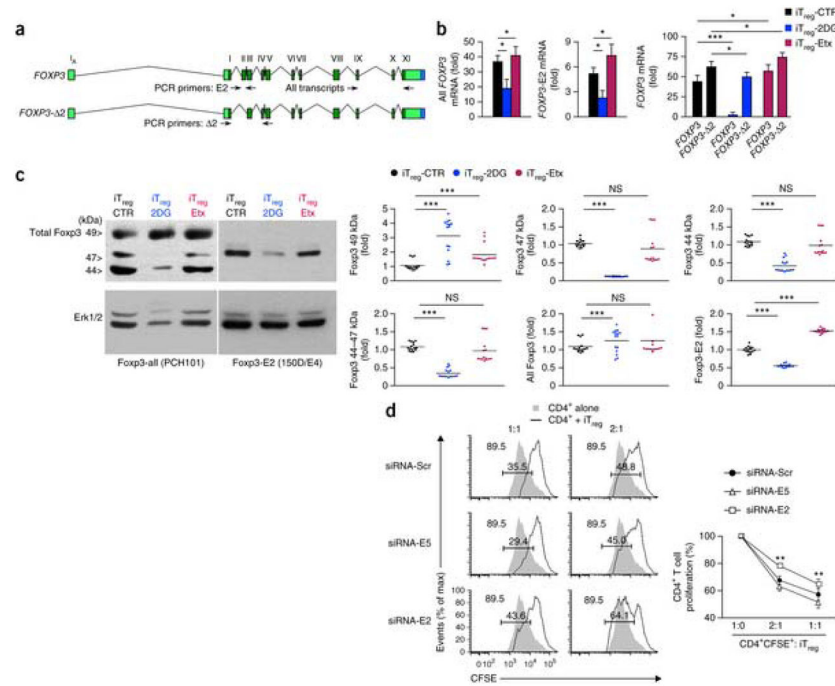
Figure 3.
Biochemical analysis of human iT_reg cells. Immunoblot analysis (far left) of total and/or phosphorylated (p-) S6, enolase-1, STAT3, STAT5, Foxp3 and Erk1/2 in iT_reg-CTR, iT_reg-2DG and iT_reg-Etx cells (above blots) left unstimulated (−) or stimulated (+) for 1 h with mAb to CD3 plus mAb to CD28 (α-CD3 + α-CD28; above lanes); total Foxp3 was assessed with mAb PCH101, which recognizes all splicing variants of Foxp3 (left margin, molecular sizes). Right, densitometry analysis, with each phosphorylated protein normalized to its total form (S6, STAT3 and STAT5), or total protein normalized to total Erk1/2 (enolase-1 and Foxp3), presented relative to results obtained for unstimulated iT_reg-CTR cells. Each symbol (right) represents an individual data point ($n = 9$); small horizontal lines indicate the mean. $*P < 0.0001$ and $**P < 0.05$ (two-tailed Student's t-test). Data are from one experiment representative of three independent experiments (far left) or three independent experiments with technical triplicates (right).

Figure 4.
Phenotypical characterization and metabolic programs of iT$_{reg}$-CTR, iT$_{reg}$-2DG and iT$_{reg}$-Etx cells. (**a**) Flow cytometry analyzing the expression of CD25 and CD4 in iT$_{reg}$-CTR, iT$_{reg}$-2DG and iT$_{reg}$-Etx cells (far left) and of T$_{reg}$ cell–specific markers (horizontal axes) (right). Numbers adjacent to outlined areas (far left) indicate percent CD25^{hi} cells or MFI (in parentheses) of CD25; numbers in plots (right) indicate percent marker-positive cells or MFI (in parentheses) of the marker. (**b**) ECAR (left) and OCR (right) of iT$_{reg}$-CTR, iT$_{reg}$-2DG and iT$_{reg}$-Etx cells stimulated for 24 h *in vitro* with mAb to CD3 plus mAb to CD28 (in conditions as in Fig. 1a; above plots). (**c**) OCR, quantifying FAO (left), of iT$_{reg}$-CTR and iT$_{reg}$-2DG cells (left) or of iT$_{reg}$-CTR and iT$_{reg}$-Etx cells (middle), stimulated for 24 h *in vitro* (as in Fig. 1a, right), in the presence of palmitate alone or palmitate plus inhibitor (as in Fig. 1b), and FAO index (right; calculated as in Fig. 1b). *P < 0.0001 and **P < 0.005 (paired two-tailed Student's *t*-test). Data are from one experiment representative of five experiments (**a**), one experiment representative of two experiments with technical duplicates (**b**; mean ± s.e.m.) or three independent experiments with technical duplicates (**c**; mean ± s.e.m. n = 18 replicates).

Figure 5.
Glycolysis controls expression of the Foxp3-E2 variants, which are indispensable for the suppressive function of iT$_{reg}$ cells. (**a**) Splicing variants of *FOXP3* mRNA: green boxes, exons (light green, 5′ and 3′ untranslated regions (UTR); dark green, coding sequence; blue, poly(A) sites); black lines, spliced regions (Δ2, deletion of exon 2); arrows, positions of PCR primers. (**b**) Real-time PCR analysis of all *FOXP3* mRNA (left) and *FOXP3*-E2 mRNA (middle) in iT$_{reg}$-CTR, iT$_{reg}$-2DG and iT$_{reg}$-Etx cells, and semiquantitative RT-PCR analysis with primers spanning exons 1–3, followed by quantification of densitometry of the PCR products *FOXP3* and *FOXP3* lacking exon 2 (*FOXP3-Δ2*) after separation by electrophoresis through agarose gels (right). (**c**) Immunoblot analysis (far left) of Foxp3 (above) and total Erk1/2 (used for normalization) in iT$_{reg}$-CTR, iT$_{reg}$-2DG and iT$_{reg}$-Etx cells, probed with mAb PCH101, to a common epitope of the amino terminus (as in Fig. 3), or mAb 150D/E4, to an epitope encoded by exon 2. Right, densitometry of all Foxp3 forms, normalized to total Erk1/2 and presented relative to results obtained for iT$_{reg}$-CTR cells. Each symbol (right) represents an individual data point (*n* = 15); small horizontal lines indicate the mean. (**d**) Proliferation (left) of CFSE-labeled CD4$^+$ T cells stimulated for 72 h *in vitro* with mAb to CD3 plus mAb to CD28 and cultured alone or in the presence of iT$_{reg}$ cells (key) generated in the presence of siRNA-E2, siRNA-E5 or siRNA-Scr (left margin), at a ratio of 1:1 or 2:1 (above plots). Numbers in plots indicate percent CFSE dilution in CD4$^+$ T cells alone (top left); numbers above bracketed lines indicate percent CFSE dilution in CD4$^+$ T cells cultured with iT$_{reg}$ cells. Right, percent proliferation of CD4$^+$ T cells in the conditions at left. *$P < 0.05$, **$P < 0.005$ and ***$P < 0.001$, siRNA-E2 versus siRNA-Scr or siRNA-E5 versus siRNA-Scr in **d** (Wilcoxon test (**b**), two-tailed Student's *t*-test (**c**) or Wilcoxon matched-pairs test (**d**)). Data are from 3 independent experiments with technical triplicates (**b**; mean ± s.d. of *n* = 9 replicates), one experiment representative of 5 experiments (**c**, far left), 5 experiments with technical triplicates (**c**, right), one experiment representative of 3

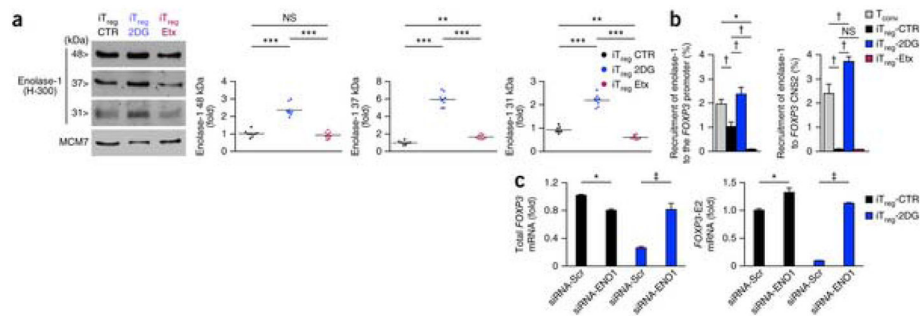experiments (**d**, left) or 3 independent experiments with 6 replicates in each (**d**, right; mean ± s.e.m. of $n = 18$ replicates).
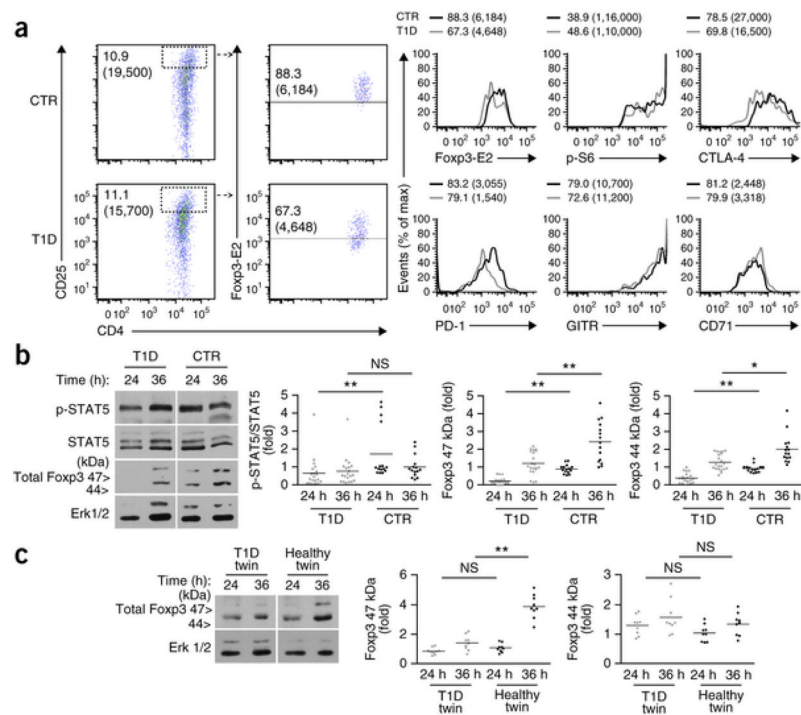
Figure 6.
Recruitment of enolase-1 to *FOXP3* regulatory regions controls Foxp3-E2 expression. (**a**) Immunoblot analysis (far left) of enolase-1 isoforms in nuclear extracts of iT$_{reg}$-CTR, iT$_{reg}$-2DG and iT$_{reg}$-Etx cells, probed with a mAb (H-300) that recognizes an epitope common to all isoforms (48, 37 and 31 kDa), and of the control protein MCM7 (bottom); gels were exposed for 1 min (48 kDa), 5 min (37 kDa) or 20 min (31 kDa) to avoid overexposure of the signal. Right, densitometry of all enolase-1 forms, normalized to MCM7 and presented relative to results obtained for iT$_{reg}$-CTR cells. Each symbol (right) represents an individual data point ($n = 9$); small horizontal lines indicate the mean. (**b**) Recruitment of enolase-1 to the promoter of *FOXP3* (left) or *FOXP3* CNS2 (right) in T$_{conv}$ cells and iT$_{reg}$-CTR, iT$_{reg}$-2DG and iT$_{reg}$-Etx cells (key), assessed by chromatin immunoprecipitation with mAb to enolase-1. (**c**) Quantitative real-time PCR analysis of all *FOXP3* transcripts (left) or *FOXP3*-E2 mRNA (right) in iT$_{reg}$-CTR and iT$_{reg}$-2DG cells generated in the presence of siRNA-Scr or siRNA-ENO1 (horizontal axis); results were normalized to those of control 18S rRNA and are presented relative to those of iT$_{reg}$-CTR cells treated with siRNA-Scr. *$P < 0.05$, **$P < 0.01$, ***$P < 0.005$, †$P < 0.001$ and ‡$P < 0.0001$ (two-tailed Student's *t*-test). Data are from three independent experiments with technical triplicates (**a**, **c**; mean ± s.e.m. of $n = 9$ in **c**) or three independent experiments (**b** mean ± s.d. of $n = 3$).
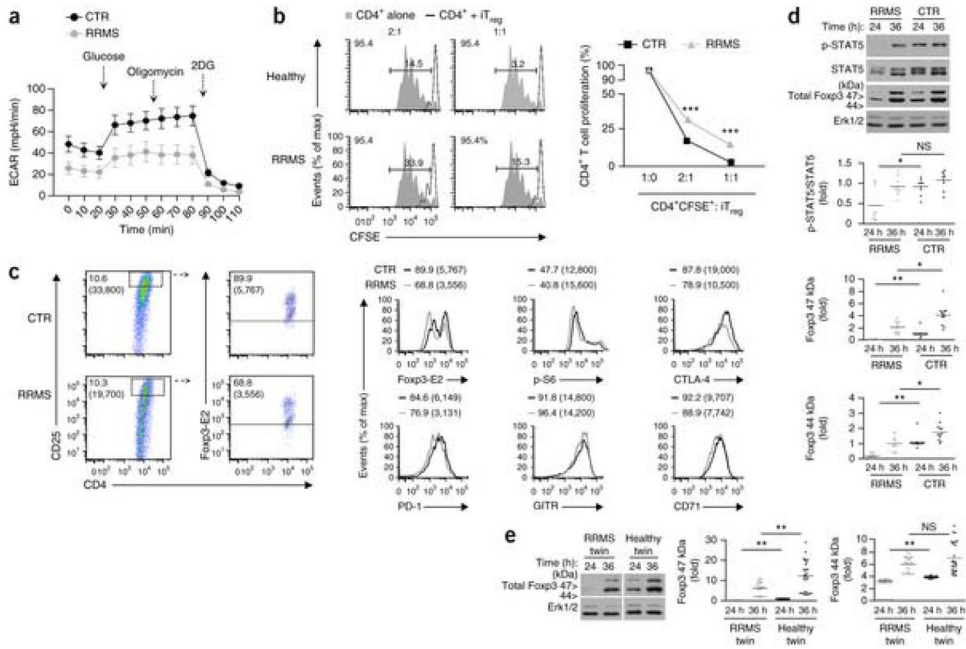
Figure 7.
Impaired glycolysis, impaired IL-2–IL-2R–STAT5 signaling and altered Foxp3-E2 expression in iT$_{reg}$ cells from subjects with RRMS. (**a**) ECAR of T$_{conv}$ cells isolated from subjects with RRMS who had not undergone treatment ($n = 6$) and healthy subjects (CTR) ($n = 14$), stimulated for 24 h *in vitro* with mAb to CD3/CD28 (in conditions as in Fig. 1a, left). (**b**) Proliferation of CFSE-labeled CD4$^+$ T cells stimulated for 96 h *in vitro* with mAb to CD3/CD28 and cultured alone or in the presence of iT$_{reg}$ cells (key) from subjects as in **a** (left margin), at a ratio of 1:1 or 1:2 (above plots). Right, percent proliferation of CD4$^+$ T cells in those conditions (far right). Numbers in plots (left) indicate percent CFSE dilution in CD4$^+$ T cells cultured alone (top left); numbers above bracketed lines indicate percent of CFSE dilution in CD4$^+$ T cells cultured with iT$_{reg}$ cells. (**c**) Flow cytometry analyzing expression of CD25, Foxp3-E2 and CD4 (left) or various T$_{reg}$ cell markers (right) in iT$_{reg}$ cells from subjects as in **a**. Numbers in top left corner indicate % CD25^{hi} cells or MFI (in parentheses) of CD25 (left) or % Foxp3-E2^{hi} cells or MFI (in parentheses) of Foxp3-E2 (middle); and numbers above plots (right) indicate % or MFI (in parentheses) of each marker. (**d**) Immunoblot analysis of phosphorylated and total STAT5 (top) and of the 44- and 47-kDa forms of Foxp3 (bottom) in T$_{conv}$ cells obtained from subjects as in **a** and stimulated for 24 or 36 h (above lanes) *in vitro* with mAb to CD3 plus mAb to CD28. Bottom, densitometry of Foxp3 normalized to total Erk1/2, or of phosphorylated STAT5 normalized to total STAT5, presented relative to results for T$_{conv}$ cells from CTR after 24 h of stimulation. Each symbol (right) represents an individual data point; small horizontal lines indicate the mean. (**e**) Immunoblot analysis (left) of the 44- and 47-kDa forms of Foxp3 in T$_{conv}$ cells obtained from pairs of monozygotic twins ($n = 6$) discordant for RRMS and without treatment, then stimulated for 24 or 36 h *in vitro* with mAb to CD3 plus mAb to CD28 (left). Right, densitometry of Foxp3 normalized to total Erk1/2 and presented relative to results obtained for T$_{conv}$ cells from the healthy twin, assessed after 24 h of stimulation.

Each symbol (right) represents an individual data point ($n = 27$); small horizontal lines indicate the mean. *$P < 0.05$, ** $P < 0.001$ and ***$P < 0.0001$ (Wilcoxon matched-pairs test (**b**) or Wilcoxon test (**d**, **e**)). Data from 6 (RRMS) or 14 (CTR) (**a**; mean ± s.e.m.), representative of 3 (**b**, left), with technical triplicates (**b**, right; mean ± s.e.m. of $n = 9$ replicates), one experiment representative of 3 experiments (**c**), one experiment representative of 4 (**d**, left), or 4 independent experiments (Foxp3) with technical triplicates from 4 subjects ($n = 12$) or 3 independent experiments (STAT5) with technical triplicates from three subjects ($n = 9$) (**d**, right), one experiment representative of 3 (**e**, left) or 3 independent experiments with nine technical replicates from 3 sets of twins (**e**, right; $n = 27$).

Figure 8.
Impaired IL-2–IL-2R–STAT5 signaling and altered Foxp3-E2 expression in iT$_{reg}$ cells from subjects with T1D. (**a**) Flow cytometry analyzing the expression of CD25, Foxp3-E2 and CD4 (left) or T$_{reg}$ cell markers (right) in iT$_{reg}$ cells from subjects with early-onset T1D or healthy subjects (CTR) (numbers in plots as in Fig. 7c). (**b**) Immunoblot analysis (far left) of phosphorylated and total STAT5 (top) and the 44- and 47-kDa forms of Foxp3 (below) in T$_{conv}$ cells obtained from subjects as in **a** and stimulated for 24 or 36 h *in vitro* with mAb to CD3 plus mAb to CD28. Right, densitometry of phosphorylated STAT5 normalized to total STAT5 or of all Foxp3 normalized to total Erk1/2, presented relative to results obtained for T$_{conv}$ cells from healthy subjects, assessed after 24 h of stimulation. Each symbol (right) represents an individual data point; small horizontal lines indicate the mean. (**c**) Immunoblot analysis of the 44- and 47-kDa forms of Foxp3 in T$_{conv}$ cells obtained from monozygotic twins ($n = 2$) discordant for T1D, then stimulated for 24 or 36 h *in vitro* with mAb to CD3 plus mAb to CD28. Right, densitometry of Foxp3 normalized to total Erk1/2, presented relative to results obtained for T$_{conv}$ cells from healthy donors, assessed after 24 h of stimulation. Each symbol (right) represents an individual data point; small horizontal lines indicate the mean. *$P < 0.005$ and **$P < 0.001$ (Wilcoxon test). Data are from one experiment representative of two (**a**), one experiment representative of three independent experiments (**b**, left), three independent experiments with technical triplicates from five healthy subjects ($n = 15$) or seven subjects with T1D ($n = 21$) (**b**, right), one experiment representative of three independent experiments (**c**, left) or three independent experiments with technical triplicates from one set of twins ($n = 9$) (**c**, right).